nature photonics

LETTERS

PUBLISHED ONLINE: 27 SEPTEMBER 2009 | DOI: 10.1038/NPHOTON.2009.169

Ultrafast waveform compression using a time-domain telescope

Mark A. Foster[1], Reza Salem[1], Yoshitomo Okawachi[1], Amy C. Turner-Foster[2], Michal Lipson[2] and Alexander L. Gaeta[1]*

Photonic systems provide access to extremely large bandwidths, which can approach a petahertz[1]. Unfortunately, full utilization of this bandwidth is not achievable using standard electro-optical technologies, and higher (>100 GHz) performance requires all-optical processing with nonlinear-optical elements. A solution to the implementation of these elements in robust, compact and efficient systems is emerging in photonic integrated circuits, as evidenced by their recent application in various ultrahigh-bandwidth instruments[2–4]. These devices enable the characterization of extremely complex signals by linking the high-speed optical domain with slower speed electronics. Here, we extend the application of these devices beyond characterization and demonstrate an instrument that generates complex and rapidly updateable ultrafast optical waveforms. We generate waveforms with 1.5-ps minimum features by compressing lower-bandwidth replicas created with a 10 GHz electro-optic modulator. In effect, our device allows for ultrahigh-speed direct 270 GHz modulation using relatively low speed devices and represents a new class of ultrafast waveform generators.

Our device, a temporal imaging system relying on temporal lenses implemented using nanofabricated silicon photonic chips, allows for the temporal compression of optical waveforms. Temporal imaging techniques are designed using the space–time duality of electromagnetic waves[5–9]. This duality arises from the isomorphism between the paraxial wave equation governing free-space diffractive propagation of a light beam and the temporal wave equation governing dispersive propagation of a light pulse. Going beyond the immediate parallels of diffraction and dispersion, the duality indicates that many spatial optical elements, for example a lens, have temporal counterparts implemented by applying the appropriate phase shift to the waveform in the time domain. It has been demonstrated that the temporal phase shift for a time lens can be realized using a nonlinear optical parametric wave-mixing process such as sum- and difference-frequency generation in $\chi^{(2)}$ materials[9,10] and more recently using four-wave mixing (FWM) in $\chi^{(3)}$ materials[2,4,11]. The use of parametric temporal imaging has predominantly been applied to the measurement of ultrafast optical waveforms by magnifying or Fourier transforming the waveform and allowing for relatively narrow bandwidth electronic measurement[2,4,10–16]. Beyond waveform characterization, parametric temporal imaging systems have the potential to generate a wide variety of ultrahigh bandwidth instruments and processors by using the wealth of knowledge developed for spatial imaging systems as a guide.

Here we apply a parametric temporal imaging system to the generation of high-bandwidth optical packets and waveforms[7] by implementing the temporal analogue of a spatial telescope. However, unlike in astronomical telescopes, the object is positioned at the front focal plane of the first lens instead of at infinity. For this reason, the device acts as an image compressor rather than an angular magnifier. An earlier non-parametric-based device demonstrated compression of 4-bit packets from 10 Gb s^{-1} to 40 Gb s^{-1} (ref. 17). This device was limited in bandwidth owing to the need to transfer the temporal amplitude in a nonlinear optical loop mirror for the lens-like element. Therefore it is restricted to the far-field limit where the amplitude profile is maintained but scaled with dispersive propagation. Through the use of a parametric time lens that transfers the amplitude and phase properties of the waveform, our technique is not restricted to this far-field regime and allows for the compression of 24-bit 10 Gb s^{-1} packets and 1.35-ns-long analog waveforms encoded using standard 10-GHz electro-optic modulation to significantly higher rates (270 Gb s^{-1}) for which direct modulation is not possible. Additionally, the phase-preserving properties of the parametric time lens in a telescopic arrangement enables complete reduction of the optical waveform (both phase and amplitude). Furthermore, the use of direct time-domain guided wave encoding allows for waveform update rates that are limited only by the repetition rate of the pump laser (40 MHz in the system demonstrated here); a dramatic improvement over the otherwise impressive waveform generators that rely on spatially and/or spectrally dispersing the lightwave, which have typical maximum update rates of 10 kHz (refs 18–22).

The critical component to the time-domain telescope is the temporal lens, which we implement using FWM in silicon nanowaveguides[2,4,11]. The high degree of optical confinement of silicon waveguides and the large material nonlinearity of silicon allows the application of nonlinear optical processes with low optical peak powers that are typically ~100 mW, and in some cases as low as 1 mW (refs 23–26). Furthermore, this waveguide confinement enables the phase velocities of interacting waves to be dramatically modified[23,27–29]; when combined with the short (~1 cm) interaction lengths, this allows for phase-matching over operating bandwidths greater than 100 nm and wide (>30 nm) pump wavelength tunability[25]. Additionally, a unique feature of FWM is that all of the interacting waves have similar photon energy, which enables the converted waveform to be generated with a similar wavelength to the pump and signal waves. The combination of these properties makes silicon FWM chips ideal devices for the implementation of a versatile parametric time lens. In particular the ability to keep all the interacting waves in the telecommunications bands is critical to the development of complex temporal imaging systems—such as the temporal telescope discussed here—which rely on a system of time lenses instead of a single lens.

A simplified depiction of the device is shown in Fig. 1a. The imaging system consists of two temporal lenses of different focal

[1]School of Applied and Engineering Physics, Cornell University, Ithaca, New York 14853, USA, [2]School of Electrical and Computer Engineering, Cornell University, Ithaca, New York 14853, USA. *e-mail: alg3@cornell.edu

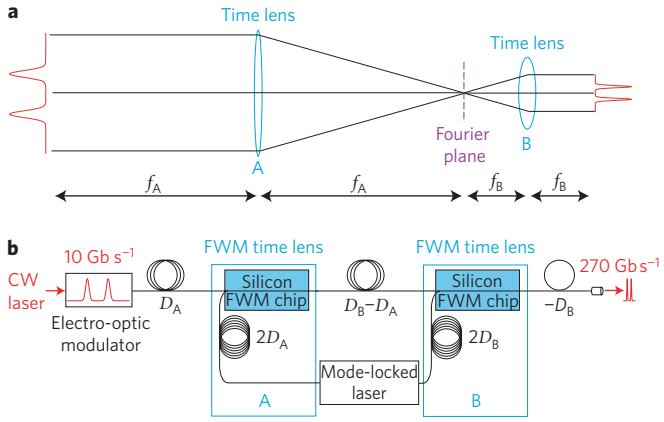

Figure 1 | Temporal telescopic system. a, Simplified spatial analogue. **b**, Detailed schematic of our temporal system in which compression occurs over two stages. During the first stage, the packet's temporal profile is converted to the frequency domain through time-to-frequency conversion using the two-focal-length temporal imaging system of lens A. The inverse Fourier transform of the packet is then performed via frequency-to-time conversion using the second lens B. The ratio of the focal lengths of the two lens systems determines the temporal compression factor. f_A (D_A) and f_B (D_B) are the spatial focal lengths (temporal dispersive focal lengths) of lenses A and B, respectively.

lengths, effectively configured to form a telescopic system. The encoded data packet is injected one focal length from the first time lens such that the Fourier transform of the waveform is generated at the opposite focal plane through the process of time-to-frequency conversion[2,12]. This Fourier plane is simultaneously positioned one focal length away from the second lens such that at the opposite focal plane of the second lens the Fourier transform of the waveform is once again generated, reversing the effect of the first lens and returning the temporal encoding to the time domain. Similarly to the angular magnification power of a spatial telescope, the compression factor depends on the relative focal lengths of the two lenses, with the amount of compression simply equal to the ratio of these lengths. For the system investigated here, the first focal length corresponds to 20 km of standard single-mode optical fibre (SMF-28), and the second focal length corresponds to 750 m of SMF-28, which yields a compression factor of 27. Although temporal compression could also be achieved using a single lens, the use of a two-lens scheme is essential for the generation of a bandwidth-limited compressed waveform.

A detailed depiction of the temporal telescope is shown in Fig. 1b. Light from a continuous-wave (CW) laser tuned to a wavelength of 1,580 nm is sent through an electro-optic modulator, and either a 24-bit, 10 Gb s^{-1} non-return to zero (NRZ) data packet or a 1.35-ns-long analog waveform is encoded. This packet is sent through a dispersion-compensating module (DCM) designed to compensate for 20.2 km of SMF-28 using approximately 4 km of normal group-velocity dispersion fibre. The dispersed packet is combined with 7-nm-bandwidth ultrafast pulses from a mode-locked fibre laser, which have been dispersed through two of the 20.2-km compensation DCMs. The packet and pump pulses are amplified and injected into the silicon nanowaveguide where they undergo FWM. The optical powers are maintained at a low enough level to avoid aberrations in the temporal lens arising from self- and cross-phase modulation, which results in negligible generation of free carriers arising from two-photon absorption. As a result, the conversion efficiency of the FWM lens is kept to approximately −10 dB. A typical spectrum showing the time-to-frequency transformation of this first temporal lens is shown in Fig. 2a. After the waveguide, the converted waveform is spectrally isolated.

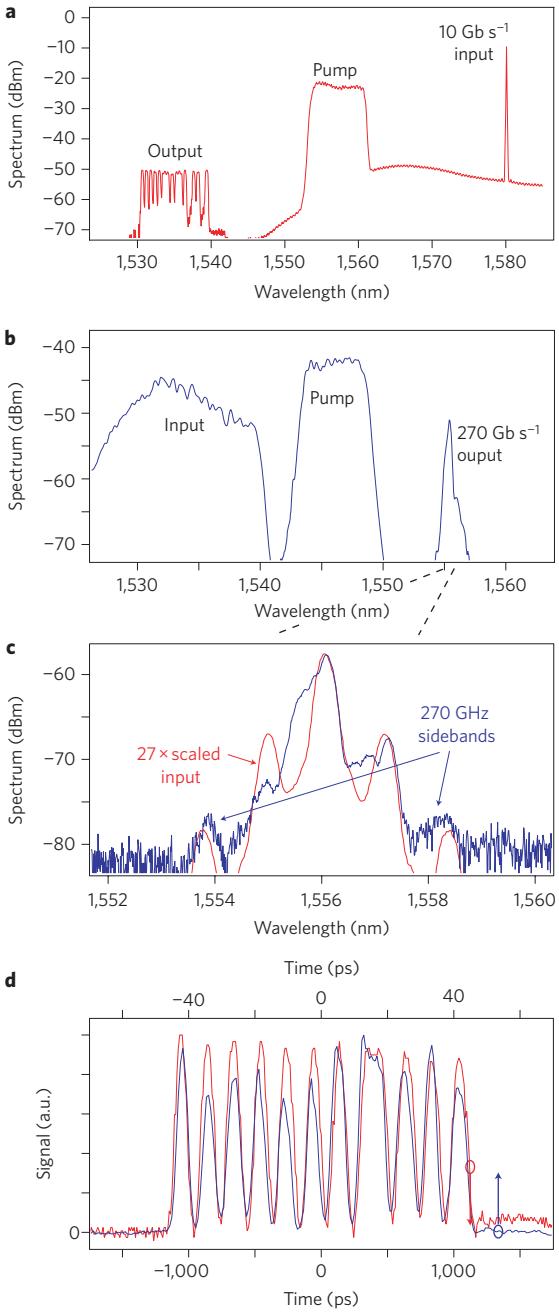

Figure 2 | Spectral and temporal outputs at different points in the temporal telescope. a, The spectrum exiting the first temporal lens showing the time-to-frequency transformation. The temporal shape of the encoded 10 Gb s^{-1} packet is visible as the spectral shape of the converted 1,535-nm output. **b**, The spectrum exiting the second temporal lens. The spectrally encoded packet is converted back to the time domain with a compressed data rate of 270 Gb s^{-1}. **c**, An expanded view of the 270 Gb s^{-1} packet spectrum (blue) with a comparison of the input spectrum shifted and scaled by 27 for comparison (red). **d**, Example original (red) and compressed (blue) waveforms overlaid to verify consistent compression across the packet.

This converted waveform is then sent though 19.45 km of SMF-28 and combined with a second 5 nm pump pulse that has been dispersed using a DCM designed to compensate for 750 m of SMF-28 using approximately 150 m of dispersion-compensating fibre. The pump and packet pulses are amplified and undergo FWM in a second silicon nanowaveguide. A typical spectrum showing the

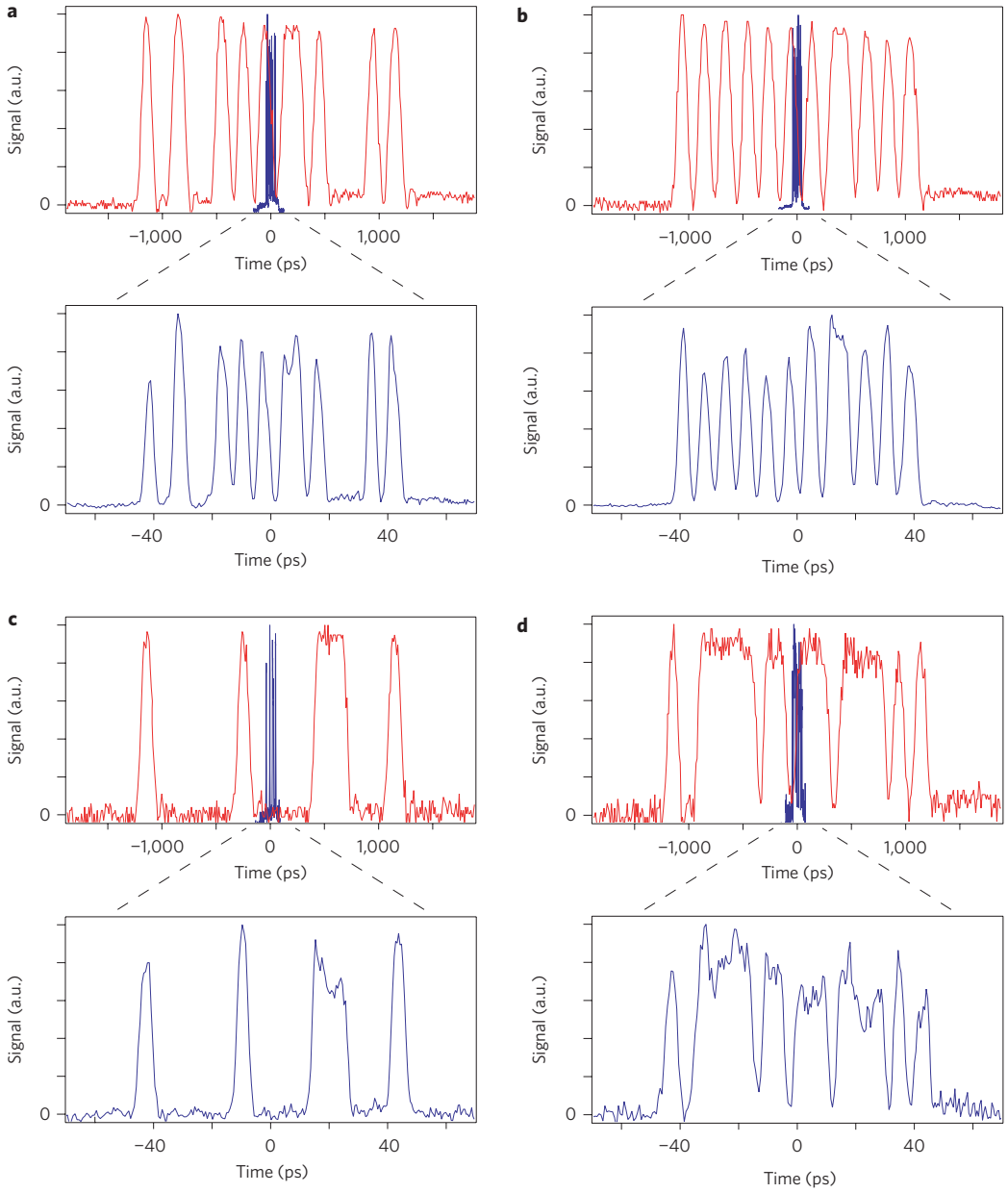

Figure 3 | Experimental demonstration of compression of 24-bit, 10 Gb s^{-1} packets to 270 Gb s^{-1}. a-d, 24-bit NRZ packets are encoded at 10 Gb s^{-1} using standard modulation technology and compressed to 270 Gb s^{-1}. The top row shows the original 24-bit 10 Gb s^{-1} packets (red) and compressed 270 Gb s^{-1} packets (blue) on the same temporal scale. The bottom row shows an expanded view of the compressed packets. The bit sequences are: **a**, (100100010101011010000101); **b**, (010101010101010110101010); **c**, (100000000100000011100001); and **d**, (100111110110111011110101).

frequency-to-time transformation of this second temporal lens is shown in Fig. 2b. The converted wave centred at 1,556 nm (Fig. 2c) is spectrally isolated and sent through 750 m of SMF-28, yielding the compressed waveform. Whereas the output spectrum (Fig. 2c) is slightly distorted, the compressed waveform is nearly bandwidth-limited as seen in the comparison between the output spectrum (blue) and the input spectrum (red). For ease of comparison the input spectrum has been scaled by a factor of 27 and shifted from 1,580 nm to 1,556 nm. The peak power in the compressed waveform is limited to approximately 500 mW by nonlinearities in this final fibre length. This compressed waveform is characterized using cross-correlation with an ultrafast pump pulse of approximately 100 fs and is compared to the original waveform, which was characterized using a 10-GHz sampling oscilloscope. An example of an uncompressed packet (red) and compressed replica (blue) are shown in Fig. 2d. The compression factor is consistent across the packet as is evident from the 270-GHz sidebands that are observed in Fig. 2c and are also clearly shown in the overlaid waveforms in Fig. 2d.

The experimental results for compression of four different 24-bit NRZ packets are shown in Fig. 3. From left to right the bit sequences are (100100010101011010000101), (010101010101010110101010), (100000000100000011100001) and (100111110110111011110101). The top row shows the original 10 Gb s^{-1} packets (red) and the compressed 270 Gb s^{-1} packets (blue) on the same temporal scale. The bottom row shows an expanded view of the compressed packets. All 24 bits of the original NRZ packets are accurately compressed into the 90 ps packet duration. A key advantage of this compression technique is that both the amplitude and phase information is preserved and thus the compressor is not sensitive to the type of encoding format. To further demonstrate the use of this technique, we compress 1.35-ns-long analog waveforms generated using an electro-optic modulator to produce 50-ps-long

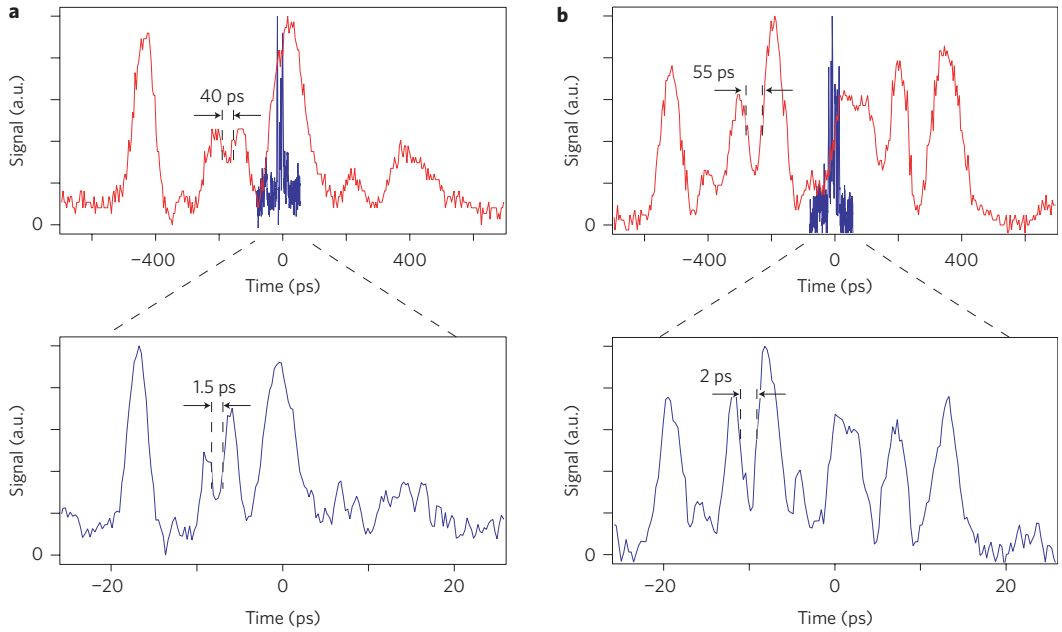

Figure 4 | Experimental demonstration of compression of analog waveforms. 1.35-ns-long analog waveforms are sent through the temporal telescope resulting in 50-ps-long compressed replicas. The top row shows the original 1.35-ns waveforms (red) and 50-ps-long compressed waveforms (blue) on the same temporal scale. The bottom row shows an expanded view (×27) of the compressed waveforms. The electro-optic modulator is driven beyond its 3-dB bandwidth yielding features less than 100 ps, which are compressed to a minimum feature size as small as 1.5 ps.

compressed replicas as seen in Fig. 4. To generate the original waveforms, we misalign the bias points of the electro-optic modulator and bandpass filter the incident electrical drive waveform, which allows the generation of complex analog waveforms with temporal features beyond the 3 dB bandwidth of the modulator. As seen in Fig. 4, features in the original waveform as short as 40 ps are transferred to the compressed waveform, resulting in a minimal compressed feature size of 1.5 ps. This indicates that the bandwidth of the compressed waveforms is limited primarily by the electro-optic modulator bandwidth and not by the temporal telescope, as expected from the >600-GHz bandwidth pump pulses used for the FWM time lenses.

In summary, we have demonstrated a time-domain telescopic system capable of compressing waveforms by a factor of 27 with a maximum compressed waveform bandwidth of greater than 270 GHz. This technique effectively allows direct 270-GHz-bandwidth modulation over the 90 ps telescopic aperture using a standard 10-GHz-bandwidth electro-optic modulator. Furthermore, both phase and amplitude information can be compressed owing to the phase preserving properties of FWM, which in principle makes the device transparent to the modulation format (that is, return to zero (RZ), NRZ, differential phase shift keying (DPSK)). The encoding of information purely in the time domain allows rapid waveform update rates, which are limited here by the 40 MHz repetition rate of the mode-locked pump laser and are fundamentally limited by the uncompressed temporal aperture. Larger compression factors with features beyond 1 THz and increased update rates can be expected in future systems by management of the third-order dispersion-induced lens aberrations[30] and by implementation of a higher repetition-rate pump laser. The temporal telescope demonstrated here extends the application of parametric temporal imaging systems beyond waveform characterization and clearly demonstrates the technological potential for a new class of high-data-rate sources and ultrafast arbitrary waveform generators using the principles of the space–time duality.

Received 4 June 2009; accepted 25 August 2009;
published online 27 September 2009

References

1. Dudley, J. M., Genty, G. & Coen, S. Supercontinuum generation is photonic crystal fiber. *Rev. Mod. Phys.* **78,** 1135–1184 (2006).
2. Foster, M. A. *et al.* Silicon-chip-based ultrafast optical oscilloscope. *Nature* **456,** 81–84 (2008).
3. Pelusi, M. *et al.* Photonic-chip-based radio-frequency spectrum analyser with terahertz bandwidth. *Nature Photon.* **3,** 139–143 (2009).
4. Salem, R. *et al.* High-speed optical sampling using a silicon-chip temporal magnifier. *Opt. Express* **17,** 4324–4329 (2009).
5. Treacy, E. B. Optical pulse compression with diffraction gratings. *IEEE J. Quantum Electron.* **5,** 454–458 (1969).
6. Akhmanov, S. A., Vysloukh, V. A. & Chirkin, A. S. Self-action of wave packets in a nonlinear medium and femtosecond laser pulse generation. *Sov. Phys. Usp.* **29,** 642–677 (1986).
7. Kolner, B. H. & Nazarathy, M., Temporal imaging with a time lens. *Opt. Lett.* **14,** 630–632 (1989).
8. Kolner, B. H. Space-time duality and the theory of temporal imaging. *IEEE J. Quantum Electron.* **30,** 1951–1963 (1994).
9. Bennett, C. V. & Kolner, B. H. Principles of parametric temporal imaging—Part I: System configurations. *IEEE J. Quantum Electron.* **36,** 430–437 (2000).
10. Bennett, C. V., Scott, R. P. & Kolner, B. H. Temporal magnification and reversal of 100 Gb/s optical data with an upconversion time microscope. *Appl. Phys. Lett.* **65,** 2513–2515 (1994).
11. Salem, R. *et al.* Optical time lens based on four-wave mixing on a silicon chip. *Opt. Lett.* **33,** 1047–1049 (2008).
12. Kauffman, M. T., Banyal, W. C., Godil, A. A. & Bloom, D. M. Time-to-frequency converter for measuring picosecond optical pulses. *Appl. Phys. Lett.* **64,** 270–272 (1994).
13. Bennett, C. V. & Kolner, B. H. Upconversion time microscope demonstrating 103x magnification of femtosecond waveforms. *Opt. Lett.* **24,** 783–785 (1999).
14. Mouradian, L. K., Louradour, F., Messager, V., Barthelemy, A. & Froehly, C. Spectro-temporal imaging of femtosecond events. *IEEE J. Quantum Electron.* **36,** 795–801 (2000).
15. Han, Y., Boyraz, O. & Jalali, B. Tera-sample per second real-time waveform digitizer. *Appl. Phys. Lett.* **87,** 241116 (2005).
16. Okawachi, Y. *et al.* High-resolution spectroscopy using a frequency magnifier. *Opt. Express* **17,** 5691–5697 (2009).
17. Almeida, P. J., Petropoulos, P., Thomsen, B. C., Ibsen, M. & Richardson, D. J. All-optical packet compression based on time-to-wavelength conversion. *IEEE Photon. Technol. Lett.* **16,** 1688–1690 (2004).
18. Weiner, A. M. Femtosecond pulse shaping using spatial light modulators. *Rev. Sci. Instrum.* **71,** 1929–1960 (2000).
19. Dugan, M. A., Tull, J. X. & Warren, W. S. High-resolution acousto-optic shaping of unamplified and amplified femtosecond laser pulses. *J. Opt. Soc. Am. B* **14,** 2348–2358 (1997).

20. Leaird, D. E. & Weiner, A. M. Femtosecond direct space-to-time pulse shaping. *IEEE J. Quantum Electron.* **37,** 495–504 (2001).
21. Chou, J., Han, Y. & Jalali, B. Adaptive RF-photonic arbitrary waveform generator. *IEEE Photon. Technol. Lett.* **15,** 581–583 (2003).
22. Willits, J. T., Weiner, A. M. & Cundiff, S. T. Theory of rapid-update line-by-line pulse shaping. *Opt. Express* **16,** 315–327 (2008).
23. Foster, M. A. *et al.* Broad-band optical parametric gain on a silicon photonic chip. *Nature* **441,** 960–963 (2006).
24. Lin, Q., Zhang, J., Fauchet, P. M. & Agrawal, G. P. Ultrabroadband parametric generation and wavelength conversion in silicon waveguides. *Opt. Express* **14,** 4786–4799 (2006).
25. Foster, M. A., Turner, A. C., Salem, R., Lipson, M. & Gaeta, A. L. Broad-band continuous-wave parametric wavelength conversion in silicon nanowaveguides. *Opt. Express* **15,** 12949–12958 (2007).
26. Turner, A. C., Foster, M. A., Gaeta, A. L. & Lipson, M. Ultra-low power parametric frequency conversion in a silicon microring resonator. *Opt. Express* **16,** 4881–4887 (2008).
27. Dulkeith, E., Xia, F., Schares, L., Green, W. M. J. & Vlasov Y. A. Group index and group velocity dispersion in silicon-on-insulator photonic wires. *Opt. Express.* **14,** 3853–3863 (2006).
28. Turner, A. C. *et al.* Tailored anomalous group-velocity dispersion in silicon channel waveguides. *Opt. Express* **14,** 4357–4362 (2006).
29. Foster, M. A., Turner, A. C., Lipson, M. & Gaeta A. L. Nonlinear optics in photonic nanowires. *Opt. Express* **16,** 1300–1320 (2008).
30. Bennett, C. V. & Kolner, B. H. Aberrations in temporal imaging. *IEEE J. Quantum Electron.* **37,** 20–32 (2001).

Acknowledgements

This work was supported by DARPA through the optical arbitrary waveform generation program and by the Center for Nanoscale Systems, supported by the NSF and the New York State Office of Science, Technology and Academic Research.

Author contributions

M.A.F., R.S., and Y.O. performed the experiments. M.A.F conceived of the compressor design. A.C.T. and M.A.F. designed the photonic chips. A.C.T. fabricated the photonic chips. M.A.F. and A.L.G prepared the manuscript. A.L.G. and M.L. supervised the project.

Additional information

Reprints and permission information is available online at http://npg.nature.com/reprintsandpermissions/. Correspondence and requests for materials should be addressed to A.L.G.